Easy-to-implement measurement method for the energy dissipated on board train with uncertainty estimation

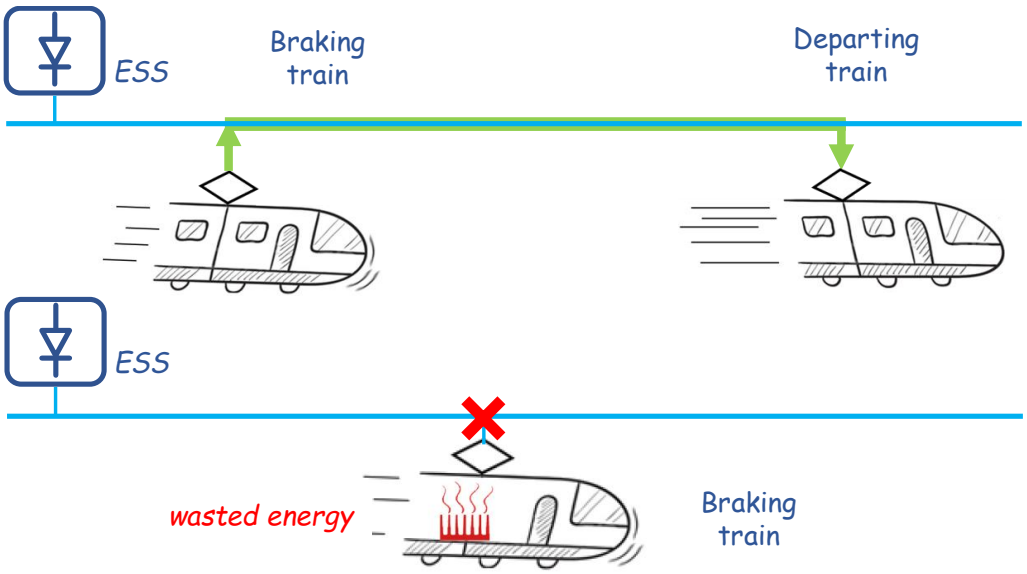

Graphical Abstract

Easy-to-implement measurement method for the energy dissipated on board train with uncertainty estimation

Antonio Delle Femine, Daniele Gallo, Domenico Giordano, Davide Signorino

Highlights

Easy-to-implement measurement method for the energy dissipated on board train with uncertainty estimation

Antonio Delle Femine, Daniele Gallo, Domenico Giordano, Davide Signorino

- Recovering braking power of trains allow to improve the efficiency of the rail system.
- Quantifying amount of energy recoverable is fundamental to dimension unconventional substations.
- A simplified method for accurate energy measurement of pulsed waveforms is developed.
- This method achieves accurate results using instrumentation already present on trains.
- The analytical model and an in-depth uncertainty analysis are presented.

Easy-to-implement measurement method for the energy dissipated on board train with uncertainty estimation

Antonio Delle Femine[a], Daniele Gallo[a], Domenico Giordano[b], Davide Signorino[b]

[a] *Universita' della Campania:"Luigi Vanvitelli", Via Roma, Aversa, 81031, Italy*
[b] *Inrim, Via Strada delle Cacce 91, Torino, 10135, Italy*

Abstract

In the near future, the railway is seen as the most important solution for reducing greenhouse gas emissions due to transportation. Investment in this sectors are ongoing, in order to increase both the level of service and energy efficiency. The adoption of recent technological solutions, as storage systems or reversible substations, could foster the efficiency, increasing the capability of recovering braking energy. The braking energy is very difficult to measure, it requires installing expensive measurement systems on board trains. In a previous paper the authors already faced this issue developing an accurate technique usable off-line. In the present paper a simplified method, easy to be implemented on train control unit, based only on already available data, is proposed. The paper describes the phenomena of interest and related measurement issues. The analytical model for the power measurement together with a deep analysis on the input quantities are presented. The uncertainty analysis of the proposed method is presented and the uncertainty budget is performed on a real test case. The metrological performances of the method show suitable accuracy level for train energy management.

Keywords: Power and Energy measurement, Railway, Braking Rheostat, Wasted Energy, Chopped Waveforms, Power Electronics, Uncertainty

1. Introduction

The transport sector, in particular road vehicles, is responsible for almost one quarter of Europe's greenhouse gas emissions. Even though a modal shift to public transport with electric rail as a backbone (urban rail in urban areas)

is a self-evident priority, the share of passenger rail in EU land transport (in passenger km) only increased from 7.0% to 7.6% between 2007 and 2016. This scenario must necessarily change, as foreseen by EU commission, thanks to the policy in supporting the development of sustainable and smart mobility [1]; as a consequence, an increase of the energy consumption for the electric rail is expected.

The need of sustainability has triggered the need to further improve the energy efficiency of rail systems. From this point of view, a present weakness of DC railway systems, that represents the most used supply system in urban areas, is the limited recovery of the electric energy generated during the dynamic braking of the trains. The relevance of dynamic braking and the description of regenerative and dissipative braking are discussed in [2, 3]. Estimates show that a train for commuter service, running on a flat route 120 km long, dissipates about 200 kWh on the braking rheostats [4]. Considering about 15 trains running on this line per day, an amount of 1 GWh per year, about the annual consumption of 365 families, is wasted for this one single commuter line. The scientific community together with railway stakeholders pays great attention to the new solutions to save braking energy. The design and implementation of new supply architectures as reversible substations that are able to inject the energy to the upstream AC grids are presented in [5, 6]. Alternative or integrating solutions like storage systems on-board and/or in substation [7, 8, 9] can collect and store the braking energy. Moreover, energy control strategies are underway for the identification of the optimal speed profile [10] and the cooperation among braking and absorbing of multiple trains [11, 12, 13], in order to maximize the recovery of extra-energy produced by the braking stage of trains. Almost all the research works cited are based on circuit simulations; very few experimental results are available in literature. It is very important to collect measurements on field, as valuable tool to assess all these research activities. Moreover such information is valuable for the designers aimed at improving the energy efficiency of the whole railway system, e.g. for dimensioning and positioning of storage systems and/or reversible substations.

Measuring energy dissipated during braking is not trivial; the involved signals are pulsed with high frequency content and high levels of amplitude. This entails the adoption of expensive measurement instrumentation [14], in particular it requires large bandwidth transducers and high performance digitizers. The diagnostic system, commonly installed on board trains, already measure some electrical quantities. These measurements are not suitable for

a complete analysis of the energy flows. Typically, not all the needed electrical quantities are acquired, and the sampling frequency is too low (a few tens of hertz) for the dynamic of involved signals. Railway operators consider the cost benefit ratio for this measurement too high. Moreover, they often completely forgo measurement of dissipated energy and prefer estimation based on mechanical assessment affected by high uncertainty. As a consequence, a low cost, accurate and easy to implement solution to measure energy dissipated during braking is needed. Nevertheless, to the best authors' knowledge, currently no article specifically faces pulsed energy measurement needs. The rigorous approach for the determination of braking energy has been addressed in [15]. It is based on the compensation of the current transducer frequency response and the stray inductance of the braking rheostat.

The authors propose a low-cost approach that allows to accurately determine the dissipated energy relying on information provided by the already installed systems, thus making easy the implementation in to traction units operating in commercial services. This new method allows the determination of wasted energy avoiding the acquisition of pulsed signals. The activities on the reliability assessment of the proposed method and statistical information on the input data of the model have been carried out thanks to the huge amount of data provided by [4]. Long measurement campaigns carried out on-board the DC 3 kV E464 locomotive, widely used for Italian commuter transport, has been performed [16]. The paper is organized as follows: Section 2 introduces the involved phenomena and measurement issues. Section 3 presents the measurement model and possible approximations. Starting from field measurements, an analysis of the input quantities is conducted in Section 4. Section 5 hosts the uncertainty analysis and the uncertainty budget associated with the proposed approach for the estimation of power during braking.

2. Description of dynamic braking

To stop a train, its kinetic energy must be removed. This task can be accomplished by dissipating the kinetic energy or by converting it into another form of energy. The most common type of braking in railway electric traction units is the dynamic braking, that is a regenerative braking system [17]. First of all, it allows to avoid mechanical braking which is subject to wear (leading to high maintenance cost). Moreover, when possible, it enables energy recovery by supplying on board loads (i. e. the auxiliary systems) and

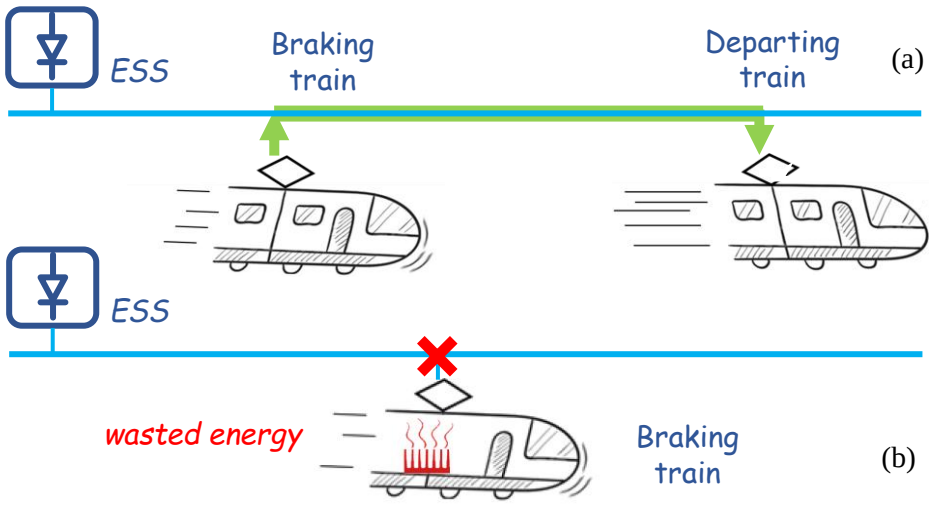

Figure 1: Energy exchange between trains (a), energy dissipation on-board (b).

injecting it back into the catenary. As described in [18], in particular for DC supplied railways, the overhead contact line is not always able to receive this energy, depending on the presence of other trains in traction simultaneously and their distance, the presence of storage systems on the line [19, 20] or the presence of reversible substations [6, 21].

Currently, the DC supply system of a railway network is obtained by means of unidirectional rectifier, that does not allow the energy flow back to the mains grid. For this reason, the energy recovered during braking can only be used by other trains on the line. When there is no other train, injection is not possible and the trains use a chopper to dissipate braking energy on the on-board rheostats bank.

In Fig. 1a two trains supplied by unidirectional Electrical Sub Station (ESS) are depicted: the one on the left is braking with a generation of energy; the other is accelerating thus recovering the braking energy from the first train. To allow the energy flow between the trains, the voltage at the pantograph of braking train rises, in order to win the resistance of the line between the two trains. In Fig. 1b the train accelerating is missing, thus the train cannot inject power on the line otherwise the voltage would rise indefinitely. In fact, when voltage exceeds a certain threshold, the braking chopper takes action dissipating all the power on board.

More in general, mixed situations can occur, in which part of the energy

can be injected and the energy surplus is dissipated on board [18]. The chopper implements a Pulse Width Modulation (PWM), so varying the duty cycle it is able to modulate the amount of the energy dissipated.

For the Italian railway system, the energy may be completely recovered only at voltages lower than 3.8 kV, over this value the on-board dissipation starts to limit the voltage increment. In details, for voltage value between 3.8 kV and 3.9 kV the train implements a mix of dissipative and regenerative braking. Above 3.9 kV, purely dissipative braking is applied to avoid further voltage rise to an unacceptable level [22].

Obviously, the installation of storage systems or reversible substations can significantly foster the energy efficiency, increasing the possibility to recover braking energy. Currently some experimental installations are ongoing in Europe [6]. For this reason, it is very important measuring the amount of energy that trains waste during braking, so as to provide valuable information for dimensioning and positioning reversible ESS or storage systems [20].

2.1. The measurement issue

Measuring the power dissipated on the braking rheostat is not trivial task. The authors experienced about installing an accurate measurement system on board [23]. The first encountered difficulty is to reach the right measurement points for the braking rheostat (typically chopper is integrated in traction cabinet that is not accessible). Moreover, the signals of interest are pulsed with high slew rate that produces high frequency content. Transducers with wide bandwith and digitizers with high sampling frequency are required.

To the best of the authors' knowledge, currently railway operators do not measure directly energy wasted during braking. They estimate it starting from available electrical and/or mechanical measured quantities. The EN50463 [24] standard prescribes the measurement of energy exchange only at the pantograph for billing. Furthermore, it establish a clustering time of 5 minute. For this reason, the majority of measurement instrumentation currently installed on-board trains, adopt a sample frequency of few tens of hertz. The characteristics of rheostat current and voltage are such as to require a sampling frequency in the order of tens of kilohertz. As stated before, the chopper switches high current levels (thousands of amperes), varying the duty cycle. To get an idea of the required measurement bandwidth, take into account that the chopper's PWM pulses can last a few hundred microseconds (e.g. duty of 3% and chopper frequency of 300 Hz).

The measurement system required to fulfill these specifications must have high performances, the cost-benefit ratio is such as to dissuade the railway operators from including it.

3. Method for the estimation of the braking rheostat energy

As stated before, a braking train tries to feed the catenary. When this is not possible, the chopper starts dissipating the energy on rheostat, by modulating it with a PWM technique. In following the paper focuses on the single PWM pulse because the braking energy is the sum of the energies dissipated by all the individual pulses.

3.1. Dissipation circuit electrical simplified model

The electrical braking system of a modern traction unit is complex [25, 26, 27]. The circuital model can be considerably simplified [15]. During braking inverter acts as a voltage generator, the braking chopper acts as a switch controlled in PWM, and rheostat absorbs and dissipates the power, acting as load. The system can be modeled as a pulsed generator that supply a resistor. Of course, the generator is not ideal (due to internal resistance, commutation time of switch) as the load (due to stray inductance). To model the dissipation process by PWM pulses, circuit of Fig. 3, is considered. It is composed by a voltage pulse generator V_{P}, that models the traction inverter (acting as generator) and the chopper switch (IGBT or GTO), a resistor R and an inductance L that model the rheostat resistance and stray inductance respectively. The results, in terms of voltage and current behaviors for a single braking chopper pulse, are also reported in the right side of Fig. 3. A duty cycle of 1% at a chopper frequency of 260 Hz with $R = 1.52\ \Omega$, and $L = 15\ \mu$H, are chosen, common values for Trenitalia locomotive E464 [16]; the electric scheme of the traction input stage is provided in Fig. 2. The picture depicts the rheostat section in red and its supply voltage, half of the catenary voltage, in green that were considered in this study.

As can be appreciated from the Fig. 3, for low values of duty cycle, the impact of the inductance is considerable, in fact the current cannot even reach its steady state value (1000A) before the end of the pulse. The duration of the pulse is shorter than the charging time of the stray inductance of the rheostat. Disregarding the stray inductance means overestimating the dissipated energy [15]. This, of course, has great impact for low duty cycles.

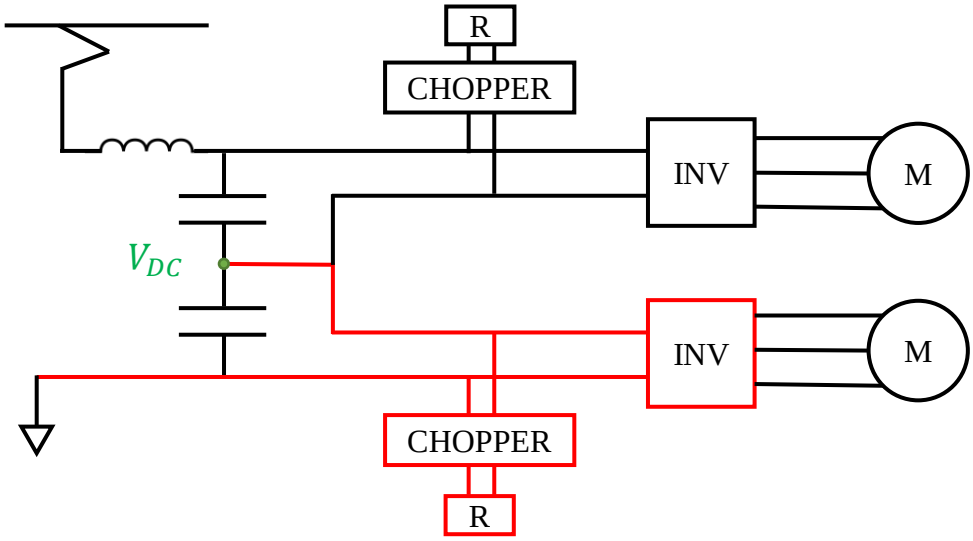

Figure 2: Electrical diagram of Trenitalia E464 input stage

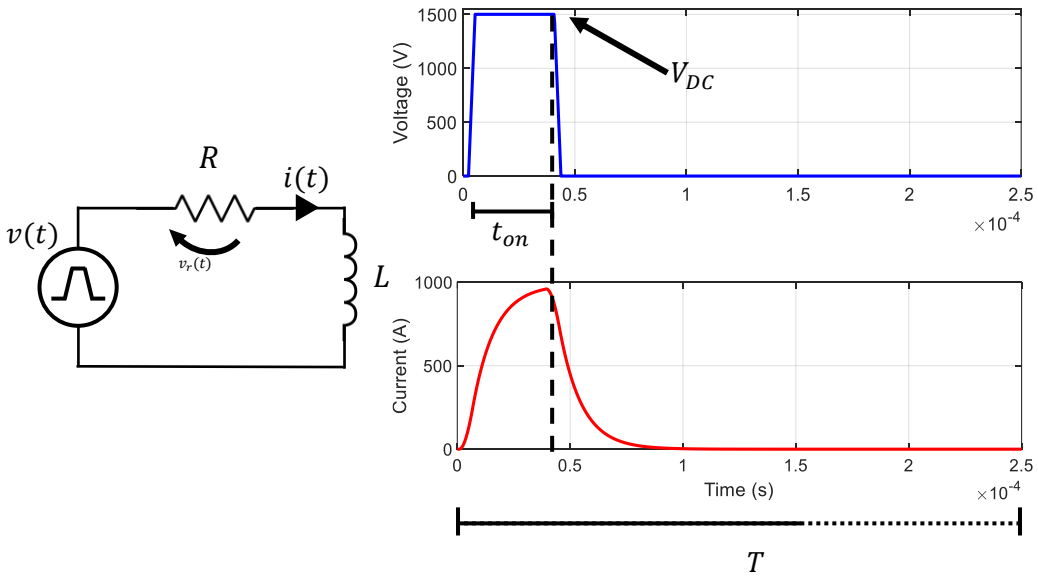

Figure 3: Circuit model and voltage an current behavior of the braking rheostat pulse

Therefore, for the energy measurement, the transient current behaviour must be taken into account.

Moreover, the commutation time of the chopper IGBT or GTO and the internal resistance of inverter and flyback diode should be considered. A simulation has been conducted to quantify the impact of the switch commutation time (typical value are few microseconds), that results negligible with respect to transient due to stray inductance, for eligible duty cycle values; the internal resistance of the active components, although negligible compared to the resistance of the rheostat, can be considered modeled by R.

3.2. Method for power wasted during braking

The present research aims to workaround the issues described in section 2.1 and to exploit the information available to the Train Control Unit (TCU). To the best of the authors' knowledge, inverter voltage measurements are already available to the railway stakeholders; moreover, it can be assumed that the duty-cycle is imposed and thus known by TCU with a good level of confidence. Pulsed voltage and current act on the braking rheostat, but at first glance, it is possible to express the dissipated power as a function of non-pulsed inverter output voltage (V_{DC}) and chopper duty cycle (δ). This way, it is possible to completely avoid the complex measurement of pulsed chopper current, which can also be affected by high uncertainty. Being aware that the TCU already measures V_{DC} and imposes δ, knowing the rheostat resistance (R), it is possible to express the dissipated power as:

$$P = V_{\mathrm{DC}}^2/R \cdot \{\delta\} \tag{1}$$

Of course, eq.1 is extremely simplified because, as clearly seen in Fig. 3, it is not possible to neglect the transient due to the stray inductance of the rheostat. This would lead to a great estimation error, as shown in [15]. The present work is focused on finding an analytic formulation that allows to reconduct the problem to a simple correction to be applied to eq.1, in order to take into account properly the transients. Considering that, as explained in previous section, the transient due to the inductance reduces the pulse power (see Fig. 3), lowering the effectiveness of the δ like it is slightly lower. This research aims to find the amount γ to subtract from δ to correctly account for this lowering, obtaining:

$$P = V_{\mathrm{DC}}^2/R \cdot \{\delta - \gamma\} \tag{2}$$

where γ is a complex function of the involved electrical quantities and will be derived in the following with a rigorous approach.

3.3. Analytic formulation of the method

The active power dissipated during a single braking chopper pulse, with reference to circuit of Fig.3, can be written as:

$$\bar{P} = \frac{1}{T} \cdot \int_0^T v(t) \cdot i(t) dt \tag{3}$$

where T is the period of the chopper, $v(t)$ and $i(t)$ are respectively voltage and current applied to the R-L series circuit. In order to simplify the computation of (3), the period T can be divided in two intervals, the first for $0 \leq t < t_{\text{on}}$ in which the electronic switch (GTO or IGBT) of the chopper is in the conductive stage, the second is defined as $t_{\text{on}} \leq t < T$ and represents the time interval in which the electronic switch is turned off (see Fig. 3). The eq. (3) can thus be written as:

$$\bar{P} = P^{'} + P^{''} = \frac{1}{T} \cdot \int_0^{t_{\text{on}}} v(t) \cdot i(t) dt + \frac{1}{T} \cdot \int_{t_{\text{on}}}^T v(t) \cdot i(t) dt \tag{4}$$

As mentioned before it is possible to neglect the commutation time of chopper, thus the voltage signal can be assumed rectangular. For the first time interval ($0 \leq t < t_{\text{on}}$) the voltage across the resistance can be expressed as:

$$v_r(t) = V_{\text{DC}} \cdot \left(1 - e^{\frac{-t}{\tau}}\right) \tag{5}$$

where V_{DC} is the voltage of the DC link which supplies the braking chopper, R is the resistance of the rheostat and τ is the time constant defined as $\tau = L/R$, and the quantity L is the stray inductance of the braking rheostat and connections. The first integral of (4) for the time interval ($0 \leq t < t_{\text{on}}$) is given by:

$$P' = \frac{1}{T} \cdot \int_0^{t_{\text{on}}} \frac{v_r(t)^2}{R} dt = \frac{V_{\text{DC}}^2}{T \cdot R} \cdot \int_0^{t_{\text{on}}} (1 - e^{(\frac{-t}{\tau})})^2 dt \tag{6}$$

The solution of the definite integral and the introduction of the chopper duty-cycle δ , defined as $\delta = \frac{t_{\text{on}}}{T}$, provides the following expression:

$$P' = \frac{V_{\text{DC}}^2}{R} \cdot (\delta - \frac{\tau}{2T} \cdot (3 + e^{-T\frac{\delta}{\tau}} \cdot (e^{-T\frac{\delta}{\tau}} - 4)) \tag{7}$$

At the time t_{on} the electronic switch is turned off, the energy accumulated in the stray inductance is dissipated by the resistance thanks to the flyback

diode. The time behavior of the voltage across the resistance $v_r(t)$, in the interval $t_{\rm on} \leq t < T$ is defined by:

$$v_r(t) = v_r(t_{\rm on}) \cdot e^{-\frac{t-t_{\rm on}}{\tau}} = V_{\rm DC} \cdot (1 - e^{(\frac{-t_{\rm on}}{\tau})}) \cdot e^{-\frac{t-t_{\rm on}}{\tau}} \tag{8}$$

$$v_r(t) = V_{\rm DC} \cdot \left(e^{\frac{t_{on}}{\tau}} - 1\right) \cdot e^{\frac{-t}{\tau}} \tag{9}$$

As a consequence, the power component P'' is defined by the relation:

$$P'' = \frac{1}{T} \cdot \int_0^T \frac{v_r(t)^2}{R} \cdot dt = \frac{V_{\rm DC}^2}{R \cdot T} \cdot (e^{\frac{t_{\rm on}}{\tau}} - 1)^2 \cdot \int_{t_{\rm on}}^T e^{-\frac{2t}{\tau}} dt \tag{10}$$

Replacing $t_{on} = \delta \cdot T$, the solution of the definite integral provides the relation:

$$P'' = \frac{V_{\rm DC}^2}{R} \cdot \left(\frac{-\tau}{2T} \cdot (-1 + e^{\frac{-2T}{\tau}(1-\delta)} + e^{-2T/\tau} - 2e^{\frac{-2T}{\tau}(1-\frac{\delta}{2})} + 2e^{\frac{-T\delta}{\tau}}\right) \tag{11}$$

By combining the two power contributions we obtain:

$$\begin{aligned} &P' + P'' = \\ &= \frac{V_{\rm DC}^2}{R} \cdot \left\{\delta - \frac{\tau}{2T} \cdot \left[2 + e^{\frac{-T\delta}{\tau}} \cdot (e^{\frac{-T\delta}{\tau}} - 2) + e^{\frac{-2T}{\tau}} \cdot (1 - e^{\frac{+T\delta}{\tau}})^2\right]\right\} \end{aligned} \tag{12}$$

This expression can be summarized as:

$$P = \frac{V_{\rm DC}^2}{R} \cdot \{\delta - \gamma\} \tag{13}$$

where γ represents the factor that corrects the systematic error introduced by the approximated model $P = \frac{P(V_{\rm DC}^2)}{R} \cdot \delta$ and is defined as:

$$\gamma = \frac{\tau}{2T} \cdot \left[2 + e^{\frac{-T\delta}{\tau}} \cdot (e^{-T\frac{\delta}{\tau}} - 2) + e^{\frac{-2T}{\tau}} \cdot (1 - e^{+T\frac{\delta}{\tau}})^2\right] \tag{14}$$

Considering that for $T = 3.85$ ms and $\tau = 10$ μs the contribution $e^{\frac{-2T}{\tau}}$ is lower than 10^{-34} the expression reported in eq (14) can be simplified as

$$\gamma = \frac{\tau}{2T} \cdot \left[2 + e^{-T\frac{\delta}{\tau}} \cdot (e^{-T\frac{\delta}{\tau}} - 2)\right] = \frac{\tau}{2T} \left[\left(e^{-T\frac{\delta}{\tau}} - 1\right)^2 + 1\right] \tag{15}$$

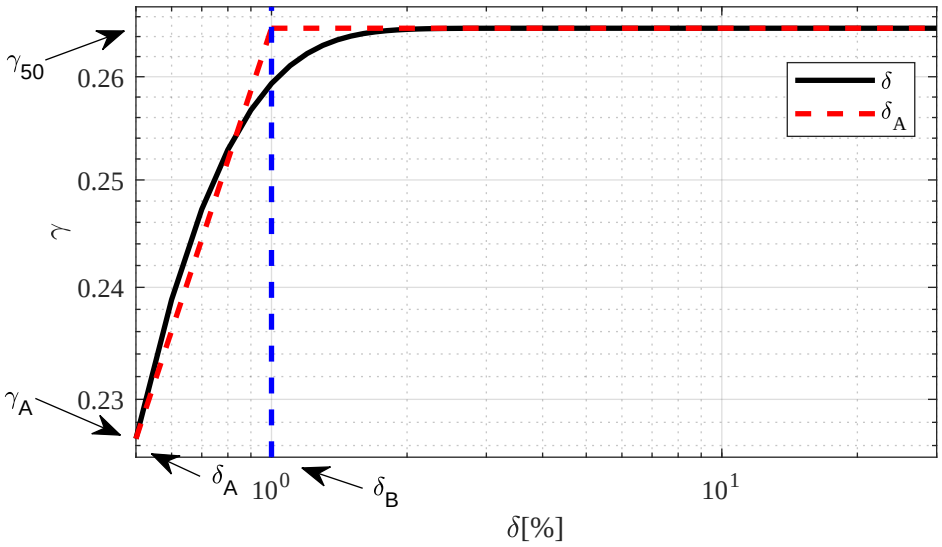

Figure 4: Actual and approximated correction factor γ versus the duty-cycle δ

For the considered case, the switching frequency is 260 Hz, thus $T = 3.85$ ms, while the rated value of the resistance R is 1.52 Ω and the estimated stray inductance L is 15 μ H, with these values, a quantification of γ is provided in the following and shown in Fig. 4. Two approximations for γ can be introduced. The first is to consider γ not dependent on the duty-cycle, approximating it with its value calculated for δ equal to 50%, that is $\gamma_{50} = 0.265\%$. This reveals to be a good approximation for duty-cycle higher than 2%.

A more accurate approximation can be introduced by the piece-wise function defined as:

$$\begin{cases} \gamma_{ap} = \gamma_A + m(log_{10}\ \delta - log_{10}\ \delta_A) & for \quad \delta_A \leq \delta < \delta_B \\ \gamma_{ap} = \gamma_{50} & for \quad \delta \geq \delta_B \end{cases} \tag{16}$$

with the angular coefficient m defined as:

$$m = \frac{\gamma_{50} - \gamma_A}{log_{10}\delta_B - log_{10}\delta_A} \tag{17}$$

The meaning of the quantities γ_A, γ_{50}, δ_A and δ_B is provided in Fig. 4. Their value, for the specific case, are summarized in Table 1.

The systematic errors associated with the determination of the dissipated power, due to a constant and a piece-wise behavior of γ are shown in Fig. 5.

Table 1: Parameter values defining the γ piece-wise approximation

Parameter	Value
γ_A	$2.25 * 10^{-3}$
γ_{50}	$2.65 * 10^{-3}$
δ_A	0.5%
δ_B	1%
m	0.00133

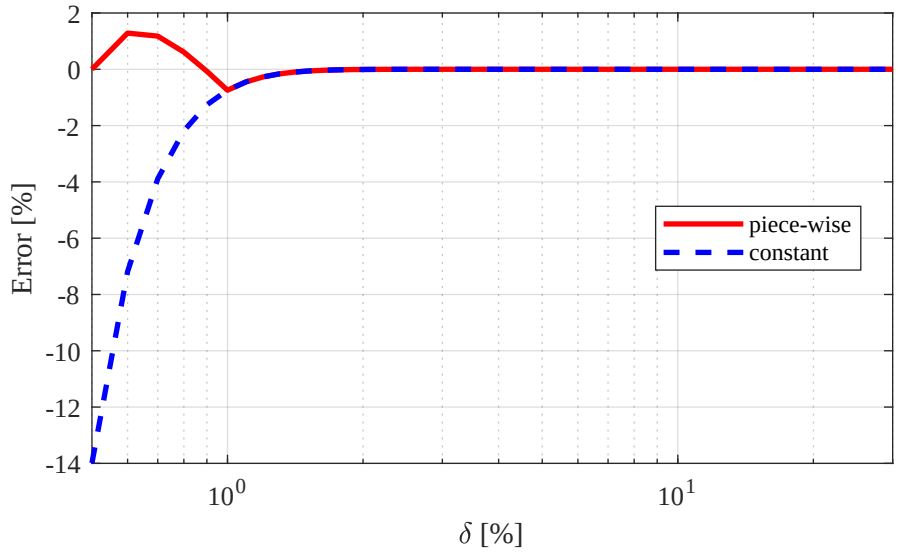

Figure 5: Error introduced by the piece-wise and constant approximation of γ vs δ

By considering a behavior of γ constant and equal to $2.65 \cdot 10^{-3}$, the maximum systematic error is of 12% at the minimum considered duty-cycle (0.5%). The error is lower than 1% for duty-cycle higher than 1%. The piece-wise approximation of γ allows to have a systematic error lower than 0.8% for all the considered duty-cycle variability (0.5% - 50%).

The method can be implemented by changing the TCU firmware in different ways. Depending on the available computation capability, it is possible to choose the complete formula through a lookup table; alternatively, one of the two proposed approximations can be chosen.

4. Input quantities estimation

In order to evaluate the metrological performance of the proposed method (13) on a real test case, the variability of all the input quantities must be evaluated. The mathematical model of the power measurement can be expressed rewriting (13) as:

$$\bar{P}(V_{\mathrm{DC}}, \delta, T, R, L) = \frac{(V_{\mathrm{DC}})^2}{R} \cdot \{\delta - \gamma(\delta, T, L, R)\} \tag{18}$$

where V_{DC}, δ, R, L and T are the input quantities. Moreover, it is necessary to estimate the impact of the uncertainties of the input quantities on the power measurement results. The quantities to be considered in the following uncertainty analysis are five: the traction inverter voltage, the rheostat resistance and inductance, the duty cycle and the chopper period. All of these will be analysed below with reference to the afore mentioned measurement campaign [16].

4.1. Traction inverter voltage

During the campaign, the inverter voltage has been monitored. The traction unit is realized with two series-connected inverters with nominal voltage of 1.5 kV. For the measurement of pulse energy, single inverter is considered.

V_{DC} is directly measured by voltage divider and a commercially available digitizer. It will be considered in the following as sources of uncertainty.

The divider used in the campaign have been calibrated at Italian National Metrology Institute (INRiM) laboratories under controlled environmental conditions (temperature of 23 $\pm$ 1° C and the humidity in 40$\div$60% range). The voltage transducer has been characterized adopting DC national standards as reference. The divider has been tested in the range 1$\div$5 kV, performing 5 intermediate step; for each step 31 iteration were implemented as prescribed by [28] in order to correctly evaluate repeatability and stability; finally the type B uncertainty of the reference system (30 μV/V) was combined too. It leads to an expanded combined uncertainty of 140 μV/V at a confidence level of 95.45% (k = 2).

Moreover, the transducer showed good amplitude linearity. In fact, the scale factor variability on the five different amplitude maintains limited within the uncertainty (140 μV/V) interval; in other words, the measured scale factors at the different amplitude levels are compatible. For this reason, the

scale factor can be considered constant with the amplitude in the range of interest.

Gain and offset of adopted data acquisition system have been determined at INRiM. The gain is known with an uncertainty of 28 μV/V at a confidence level of 95.45% ($k = 2$). The offset is -16 μV and is known with an expanded uncertainty ($k = 2$) of 3 μV. Analyzing the rheostat currents i_{R}, it has been possible to identify all the chopper pulses over all the measurement campaign. A total of 7,866,069 pulses were collected and analyzed. For each braking pulse, the average values of v_{DC} has been determined. In Fig. 6 it is depicted the PDF (Probability Density Function) and CDF (Cumulative Distribution Function) of this quantity as result of the statistical analysis carried out. The PDF shows the variability of the voltage applied to the rheostat, as a consequence of the variability of the line voltage.

As you can see, the average value of distribution coincides with half of the chopper intervention threshold, because the line voltage divides equally on the two series connected inverters. Moreover, voltage never overcome 1.95 kV, in fact, as stated before, above 3.9 kV at the pantograph, purely dissipative braking is applied to avoid further voltage increase.

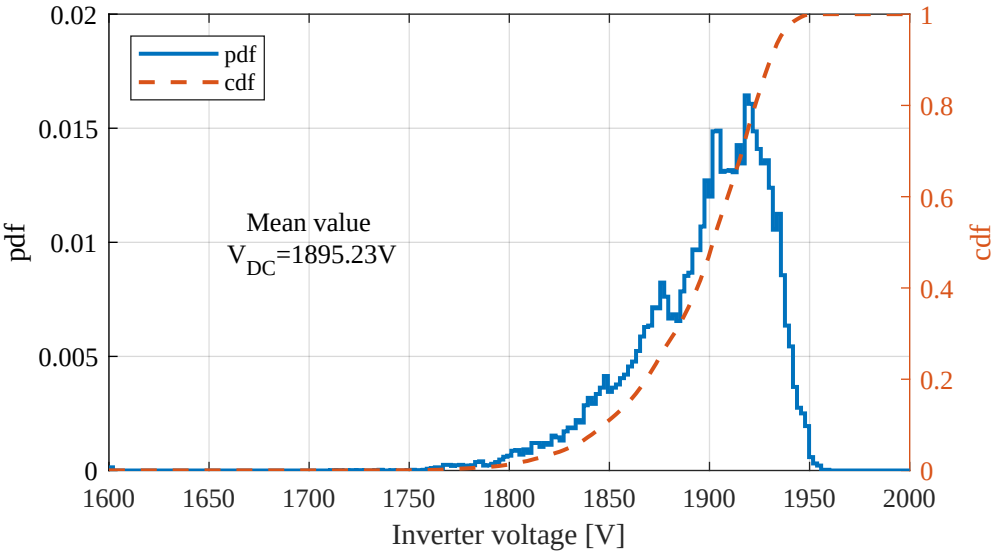

Figure 6: Statistical analysis of the inverter voltage.

4.2. Duty-cycle

Regarding the duty cycle, it is supposed to be known with a high confidence level, it is an information available to the TCU. Of course, the timebase of the TCU could present clock deviation and clock jitter due to hardware and/or firmware issues. As stated before, $\delta = \frac{t_{\mathrm{on}}}{T}$ that can be written as: $\delta = \frac{N_{\mathrm{on}} \cdot t_{\mathrm{c}}}{N_{\mathrm{tot}} \cdot t_{\mathrm{c}}} = \frac{N_{\mathrm{on}}}{N_{\mathrm{tot}}}$ where t_{c} is the clock period, N_{tot} is the number of clock pulses during a chopper period, and N_{on} is the number of clock pulses during a chopper ON time. Thus δ does not depend on the clock frequency deviation, because it is a ratio between two integer number of clock pulses.

The only source of uncertainty for duty cycle is the jitter, it is basically the uncertainty in clock edge. This means that the rising or the falling edges can occur later or sooner with respect to the desired. Nevertheless, considering that the clock frequency is very high with respect to the chopper frequency, even a great relative variation on clock edge leads to a negligible effect on duty cycle. For instance, supposing a clock frequency of 100 MHz, that means a period of 10 ns, and supposing poor clock quality that leads even to 10% variation on clock edge with respect to the clock period, the jitter will be 1 ns thus it can be neglected with respect to the chopper period that is about 3.5 ms. In conclusion the uncertainty on duty cycle due to clock jitter can be considered as little as few part per million. In Fig. 7 the PDF and the CDF of the obtained results are reported. As it can be noted the duty is never lower than 2%. This means that for the case of study, the parameter γ in (13) can be approximated as γ_{50}, and the error due to this assumption is negligible (see dashed blue line in Fig. 5 for $\delta = 2\%$). Obviously, not always this is possible; in general, for higher chopper frequency or greater rheostat inductance, this approximation can lead to an unacceptable error. At higher switching frequency or greater inductance, the error curve of Fig. 5 shifts to the right, so the same value of δ will correspond to a higher error.

4.3. Chopper period

As for the duty cycle, the chopper period also depends on the timebase of the TCU, but in this case it is directly influenced by clock deviation. Systematic error can be compensated with a clock measurement, but thermal drift of clock will still influence the period and thus the measurement of electric power with the proposed method (13). In fact, the correction coefficient γ, introduced in section 3.3, depends on the chopper period T. From a physical point of view, as expected, at the increase of T, for the same δ, the shape of the current pulse tends to be similar to the ideal case of square wave. The

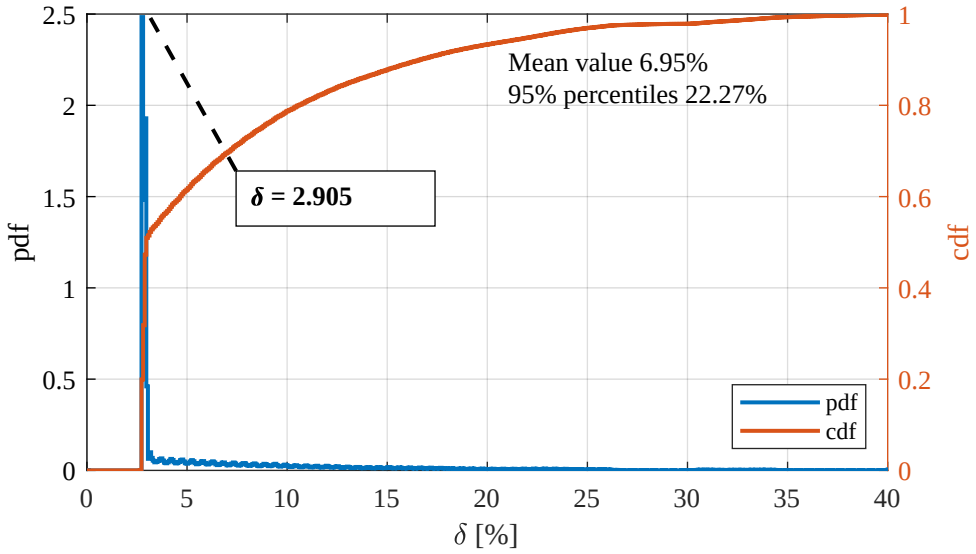

Figure 7: Statistical analysis of the chopper δ on the whole measurement campaign.

systematic error provided by the approximation of the pulse to the ideal case decreases as T increases. Instead, decreasing T rise and fall times of the exponential transient become more significant with respect to pulse duration. Thus with lower T a greater correction γ is needed. The dependency of γ with T will be considered in the following uncertainty analysis.

4.4. Rheostat resistance and inductance

The rheostat resistance is crucial for the application of the proposed method (13). Rheostat stray inductance instead influences the transient behavior of chopper current. Equation (15) takes into account this behavior. Of course, the resistance value could differ from the rated one and certainly it varies with temperature and other influence factors. This lack of information is considered as source of uncertainty. For the considered locomotive, the rated value of resistance is declared for 1.52 Ω with an accuracy of ± 5% in all operating conditions (see Table 2).

As stated before, the proposed method relies on the metrological characterization braking rheostat in terms of both resistance and inductance. During the afore mentioned measurement campaign, a laboratory calibration was not possible for the authors because the rheostat was already installed on an operating train. For this reasons, the resistance value was

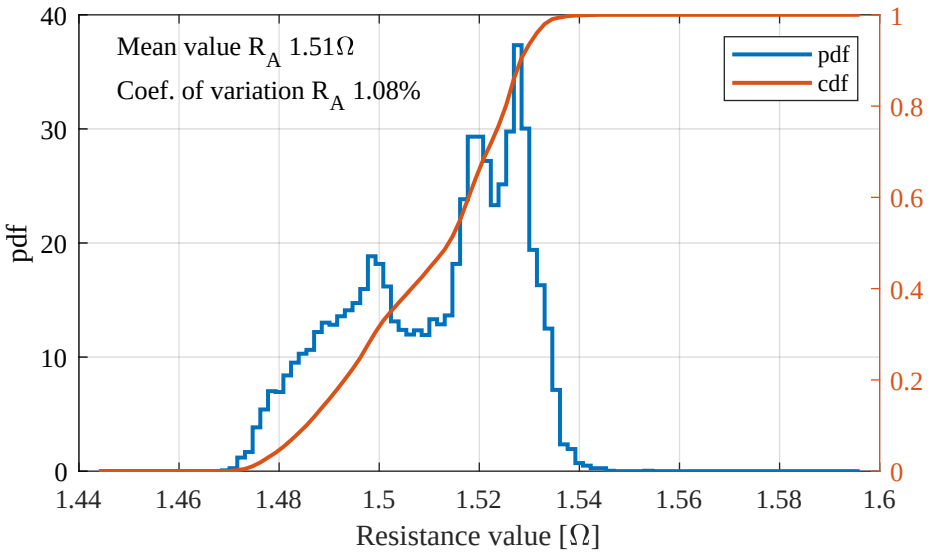

Figure 8: Statistical analysis of the rheostat resistance over all recorded braking

determined by voltage and current measurements. The rated value declared by the manufacturer for the stray inductance has been considered. The associated uncertainty, 2%, has been estimated on the base of the state of the art for what concern the on-site measurement of inductance parameter of a circuit.

As stated before, almost 8 million pulses were analysed. Fig.8 shows the PDF and CDF, together with the mean value and the Coefficient of Variation (CoV), defined as the ratio between the standard deviation and the mean value for the resistance. The classes on which the statistic is made

Table 2: Braking Rheostat Characteristics

Parameter	Value
Maximum power	1200 kW
Resistance at 20 °C	1.52 Ω
Maximum resistance variation in range [20 600] °C	5%
Operating voltage	1.5 kV
Maximum RMS current	900 A
Stray inductance	15 μH

are 100 and uniformly distributed, for values ranging from 1.52 -5% to 1.52 + 5%. The adoption of estimated mean value for R in the application of (13), greatly reduce the error on measurement of energy dissipated by the rheostat. The statistic shows how the values are concentrated in a very narrow range of occurrences, in particular the CoV is just over 1%, thus considerably less then the rated 5%, this greatly reduces the impact that resistance variation has on the performance of the proposed method.

The rated stray inductance is 15 μH. Generally speaking, stray inductance depends on geometric and materials properties, in the case of study, it is possible to consider these properties as almost invariant, or at least neglect their effect.

5. Uncertainty analysis on the estimated energy

Assuming that all input quantities in eq. 18 are independent [28], it is possible to obtain the combined standard uncertainty u_c by propagating the standard uncertainties of the three inputs quantities on the power:

$$u_c(P)^2 = \left(\frac{\partial P}{\partial V_{DC}} \cdot u(V_{DC})\right)^2 + \left(\frac{\partial P}{\partial \delta} \cdot u(\delta)\right)^2 + \left(\frac{\partial P}{\partial T} \cdot u(T)\right)^2 + \left(\frac{\partial P}{\partial R} \cdot u(R)\right)^2 + \left(\frac{\partial P}{\partial L} \cdot u(L)\right)^2 \tag{19}$$

5.1. Voltage measurement contribution

In order to estimate uncertainty on the inverter voltage measurement, gain and offset of the data acquisition system, and scale factor of voltage divider, must be taken into account. The measurement model for quantity V_{DC} in (18), can be written as:

$$V_{DC} = [k_{div} \cdot k_{daq} \cdot (V_{LV} - V_{OFF})] \tag{20}$$

where k_{div} is the voltage divider scale factor, k_{daq} and V_{OFF} are the scale factor and the offset of data acquisition system respectively, V_{LV} is the average of readings provided by the data acquisition system, performed over a single pulse and can be written as:

$$V_{LV} = \frac{1}{N} \sum_{k=1}^{N} v[k] \tag{21}$$

where v[k] is k-th sample and N is the number of samples acquired during a chopper period.

Defining V'_{LV} as the difference $(V_{\mathrm{LV}} - V_{\mathrm{OFF}})$, the combined uncertainty is:

$$u_{\mathrm{c}}(V'_{\mathrm{LV}})^2 = u(V_{\mathrm{LV}})^2 + u(V_{\mathrm{OFF}})^2 \tag{22}$$

Then, the combined uncertainty associated with (20) can be easily obtained by the relative uncertainties:

$$\left(\frac{u_{\mathrm{c}}(V_{\mathrm{DC}})}{V_{\mathrm{DC}}}\right)^2 = \left(\frac{u(k_{\mathrm{div}})}{k_{\mathrm{div}}}\right)^2 + \left(\frac{u(k_{\mathrm{daq}})}{k_{\mathrm{daq}}}\right)^2 + \left(\frac{u_{\mathrm{c}}(V'_{\mathrm{LV}})}{V'_{\mathrm{LV}}}\right)^2 \tag{23}$$

In table 3 the uncertainty budget for the measurement model (20) are reported. For k_{div}, k_{daq}, and V_{OFF} data from INRIM calibration has been used (see section 4.1). Repeatability and stability for V_{LV} have been evaluated by applying a reference DC voltage to the acquisition channel. 31 iteration have been performed as prescribed by GUM [28], configuring digitizer in the same way adopted for field measurement (i.e. sampling rate of 50 kHz, integration of time of 3.85 ms, that is the chopper nominal period). The relative combined standard uncertainty obtained from equation (22) and (23) have been reported on the last raw of the table 3. The monitoring of the temperature

Table 3: Uncertainty budget for voltage

source	u
k_{div}	$70\mu V/V$
k_{daq}	$14\mu V/V$
V_{OFF}	$3\mu V$
V_{LV}	$7\mu V$
V_{DC}	$71\mu V/V$

inside the locomotive high voltage cabinet, performed during the measurement campaign, provides a limited range of variation, $[18\ 23]°C$. Thanks to this temperature stability, the uncertainties obtained in the laboratory are kept constant for in field measurement. With reference to (19), this uncertainty on voltage measurement must be weighted by partial derivative of P with respect to voltage:

$$\frac{\partial P}{\partial V_{\mathrm{DC}}} = 2 \cdot \frac{V_{\mathrm{DC}}}{R} \cdot (\delta - \gamma) \tag{24}$$

5.2. Duty Cycle contribution

As stated in section 4.2, even if it is supposed to be known, duty-cycle can be affected by uncertainty due to clock jitter. Thus the uncertainty $u(\delta)$ weighted by partial derivative of P with respect to δ:

$$\frac{\partial P}{\partial \delta} = \frac{V_{\mathrm{DC}}^2}{R} \cdot \left(1 - \frac{\partial \gamma}{\partial \delta}\right), \quad \text{where :} \quad \frac{\partial \gamma}{\partial \delta} = e^{-T\frac{\delta}{\tau}} \cdot \left(e^{-T\frac{\delta}{\tau}} - 1\right) \tag{25}$$

As expected the impact on combined uncertainty increases for low value of δ, in particular when the product $\delta \cdot T$ is comparable to τ.

5.3. Chopper period impact on uncertainty

The dependency of P from chopper period (T) is present in γ, partial derivative is:

$$\frac{\partial P}{\partial T} = \frac{V_{\mathrm{DC}}^2}{R \cdot T} \cdot \left[\gamma - \delta \cdot e^{-T\frac{\delta}{\tau}} \cdot \left(e^{-T\frac{\delta}{\tau}} - 1\right)\right] \tag{26}$$

Note that this sensitivity is almost constant with δ. In fact the term with exponential has low influence for $\delta > 1\%$, more in general with a time constant τ at least one order of magnitude lower than chopper period T. For the same reason, γ is almost constant, moreover, for low δ, the decrease of the exponential term compensate the decrease in γ.

5.4. Resistance and inductance contributions

The rheostat resistance is explicitly present in equation (18) and implicitly in γ, see (15), inside τ, that is defined as $\tau = L/R$. The variability of R is mainly due to temperature variation by Joule effect, it has been evaluated experimentally over the whole measurement campaign (see Fig.8); the CoV of R will be considered in the following as relative standard uncertainty to take into account this effect. This uncertainty must be weighted by partial derivative of P with respect to R:

$$\frac{\partial P}{\partial R} = \frac{V_{\mathrm{DC}}^2}{R^2} \cdot \left[2\gamma - \delta + \delta \cdot e^{-T\frac{\delta}{\tau}} \cdot \left(e^{-T\frac{\delta}{\tau}} - 1\right)\right] \tag{27}$$

Note the presence of δ without the exponential term. With high value of duty cycle, great impact of resistance uncertainty is expected. Nevertheless the sensitivity decreases when δ decreases.

As mentioned before a standard uncertainty of 2% will be considered for L in the following, the sensitivity coefficient for inductance is:

$$\frac{\partial P}{\partial L} = \frac{V_{\mathrm{DC}}^2}{R^2} \cdot \left[\frac{\delta}{L} \cdot e^{-T\frac{\delta}{\tau}} \cdot \left(e^{-T\frac{\delta}{\tau}} - 1 \right) - \gamma \cdot L \right] \tag{28}$$

This coefficient reveals that L has low impact on combined uncertainty, in fact both the term in the square brackets have low numeric value.

5.5. Uncertainty budget

Starting from the analysis of the uncertainty sources, shown in the previous subsections, the uncertainty budget is quantified in table 4. It summarizes all the standard uncertainty contributions due to the considered quantities. The last row provides the relative combined standard uncertainty of the dissipated power. The budget has been computed for various value of delta ranging from 0.5% to 50% and for three voltage values: the mean and the extremes of the voltage distribution showed in Fig. 6. As expected, rheostat resistance has a dominant effect on the combined uncertainty. Chopper period and duty cycle has negligible effect, only for $\delta = 0.5\%$ uncertainty contribution almost reach 100 μW/W. Inductance uncertainty contribution becomes significant only for low value of δ. It is interesting to note that the voltage variation does not produce any effect, in fact $u_{\mathrm{c}}(P)$ depends on V_{DC}^2, but also P depends on the same quantity, thus changing the voltage level changes only the absolute uncertainty but not the relative one. Contrary to what was expected, the relative uncertainty decreases with delta. Of course the exponential terms in the equations (26, 27, 28) increase as δ decreases, in fact the corresponding uncertainties contributions due to duty cycle, chopper period and inductance increases, but the main contribution due to R, decreases, and consequently the combined uncertainty decreases too.

6. Conclusions

The authors propose an easy-to-implement and accurate methodology for the determination of power dissipated on braking rheostat of a train. The methodology is based on the measurement of the inverter voltage and the chopper duty cycle. The rated resistance and stray inductance of the braking resistor and the chopper period complete the input quantities. Models of the measurement, with different approximation levels of the correction factor that takes into account the transient behaviour of the chopped current, are

Table 4: Uncertainty budget for power

Operating Point		Relative Uncertainty Contribution [mW/W]					Standard Uncertainty
δ[%]	V_{DC}[V]	V_{DC}	δ	T	R	L	$u_{\mathrm{c}}(P)/P$ [mW/W]
50	1895	0.14	0.00	0.00	10.76	0.00	10.76
5	1895	0.14	0.01	0.00	10.33	0.00	10.34
2	1895	0.14	0.02	0.01	9.56	0.00	9.56
1	1895	0.14	0.03	0.03	8.12	0.20	8.12
0.5	1895	0.14	0.09	0.07	5.64	2.61	6.22
3	1895	0.14	0.01	0.01	10.00	0.00	10.00
3	1600	0.14	0.01	0.01	10.00	0.00	10.00
3	1900	0.14	0.01	0.01	10.00	0.00	10.00

proposed. Thanks to the relevant amount of data recorded on-field during previous measurement campaigns, it has been possible to estimate the actual variability of the resistance in real operating conditions. Such analysis has allowed a rigorous uncertainty budget determination, associated with the dissipated power estimation, with a detailed description and quantification of the uncertainty sources for each input quantity. The weight of each uncertainty contribution has been computed and discussed. Even though the methodology has been applied to a specific traction unit for 3 kV DC railway system, the model definition guarantees its applicability even for traction units with different dissipative braking architectures. The uncertainty contribution analysis shows that the main one is the resistance variability due to the Joule effect heating. An uncertainty of 1 % on the resistance value means 1 % on the estimated dissipated power at high duty cycle. The uncertainties on the supply voltage, duty cycle and chopper period can be neglected. For duty cycle values lower than 1 %, the resistance uncertainty contribution decreases and, at the same time, the uncertainty contribution provided by the stray inductance increases. The proposed method has been designed to enable railway operators to measure wasted energy accurately, without installing any additional measurement device and can be implemented with minimal expense, simply upgrading the TCU firmware.

Acknowledgment

The results here presented are developed in the framework of the 16ENG04 MyRailS Project. The latter received funding from the EMPIR program co-financed by the Participating States and from the European Union's Horizon 2020 research and innovation program.

References

[1] European Commission. Transport 2050: The major challenges, the key measures, Mar. 2011. URL ec.europa.eu/commission/presscorner/detail/en/MEMO_11_197.

[2] Lionginas Liudvinavičius and Leonas Lingaitis. Electrodynamic braking in high-speed rail transport. *Transport*, 22, 07 2007. doi: 10.1080/16484142.2007.9638122.

[3] Yuhua Wang, Jianlin Miao, and Yuanfang Wei. The research of traction motor energy-saving regenerative braking control technology. In *2010 International Conference on Intelligent Computation Technology and Automation*, volume 3, pages 930–933, 2010. doi: 10.1109/ICICTA.2010.47.

[4] EURAMET. Metrology for smart energy management in electric railway systems, 16ENG04 MyRailS, 2017.

[5] David Ramsey, Tony Letrouve, Alain Bouscayrol, and Philippe Delarue. Comparison of energy recovery solutions on a suburban dc railway system. *IEEE Transactions on Transportation Electrification*, pages 1–1, 2020. doi: 10.1109/TTE.2020.3035736.

[6] Mihaela Popescu and Alexandru Bitoleanu. A review of the energy efficiency improvement in dc railway systems. *Energies*, 12(6), 2019. ISSN 1996-1073. doi: 10.3390/en12061092.

[7] Chaoxian Wu, Shaofeng Lu, Fei Xue, Lin Jiang, and Minwu Chen. Optimal sizing of onboard energy storage devices for electrified railway systems. *IEEE Transactions on Transportation Electrification*, 6(3):1301–1311, 2020. doi: 10.1109/TTE.2020.2996362.

[8] F. Foiadelli, M. Roscia, and D. Zaninelli. Optimization of storage devices for regenerative braking energy in subway systems. In *2006 IEEE Power Engineering Society General Meeting*, pages 6 pp.–, 2006. doi: 10.1109/PES.2006.1708894.

[9] Giuliano Cipolletta, Antonio Delle Femine, Daniele Gallo, Mario Luiso, and Carmine Landi. Design of a stationary energy recovery system in rail transport. *Energies*, 14(9), 2021. ISSN 1996-1073. doi: 10.3390/en14092560.

[10] María Dominguez, Antonio Fernández-Cardador, Asunción P. Cucala, and Ramón R. Pecharroman. Energy savings in metropolitan railway substations through regenerative energy recovery and optimal design of ato speed profiles. *IEEE Transactions on Automation Science and Engineering*, 9(3):496–504, 2012. doi: 10.1109/TASE.2012.2201148.

[11] S. Goh, M. Griffith, and K. Larbi. Energy saving by using regenerating braking as normal train operation. In *IET Conference on Railway Traction Systems (RTS 2010)*, pages 1–4, 2010. doi: 10.1049/ic.2010.0041.

[12] Jingang Guo, Junping Wang, and Binggang Cao. Study on braking force distribution of electric vehicles. In *2009 Asia-Pacific Power and Energy Engineering Conference*, pages 1–4, 2009. doi: 10.1109/APPEEC.2009.4918806.

[13] Shuai Su, Xuekai Wang, Yuan Cao, and Jiateng Yin. An energy-efficient train operation approach by integrating the metro timetabling and eco-driving. *IEEE Transactions on Intelligent Transportation Systems*, 21 (10):4252–4268, 2020. doi: 10.1109/TITS.2019.2939358.

[14] Jane Lehr and Pralhad Ron. *Pulsed Voltage and Current Measurements*, pages 493–546. 2018. doi: 10.1002/9781118886502.ch10.

[15] Domenico Giordano, Davide Signorino, Daniele Gallo, Helko E. van den Brom, and Martin Sira. Methodology for the accurate measurement of the power dissipated by braking rheostats. *Sensors*, 20 (23), 2020. ISSN 1424-8220. doi: 10.3390/s20236935. URL `https://www.mdpi.com/1424-8220/20/23/6935`.

[16] G. Crotti, D. Giordano, D. Signorino, A. Delle Femine, D. Gallo, C. Landi, M. Luiso, A. Biancucci, and L. Donadio. Monitoring energy

and power quality on board train. In *2019 IEEE 10th International Workshop on Applied Measurements for Power Systems (AMPS)*, pages 1–6, 2019. doi: 10.1109/AMPS.2019.8897794.

[17] Shaofeng Lu, Paul Weston, Stuart Hillmansen, Hoay Beng Gooi, and Clive Roberts. Increasing the regenerative braking energy for railway vehicles. *IEEE Transactions on Intelligent Transportation Systems*, 15 (6):2506–2515, 2014. doi: 10.1109/TITS.2014.2319233.

[18] F. Cascetta, G. Cipolletta, A. Delle Femine, J. Quintana Fernández, D. Gallo, D. Giordano, and D. Signorino. Impact of a reversible substation on energy recovery experienced on-board a train. *Measurement*, page 109793, 2021. ISSN 0263-2241. doi: https://doi.org/10.1016/j.measurement.2021.109793.

[19] Vasilis A. Kleftakis and Nikos D. Hatziargyriou. Optimal control of reversible substations and wayside storage devices for voltage stabilization and energy savings in metro railway networks. *IEEE Transactions on Transportation Electrification*, 5(2):515–523, 2019. doi: 10.1109/TTE.2019.2913355.

[20] Giuliano Cipolletta, Antonio Delle Femine, Daniele Gallo, Mario Luiso, and Carmine Landi. Design of a stationary energy recovery system in rail transport. *Energies*, 14(9), 2021. ISSN 1996-1073. doi: 10.3390/en14092560. URL `https://www.mdpi.com/1996-1073/14/9/2560`.

[21] G. Cipolletta, A. Delle Femine, D. Gallo, C. Landi, M. Luiso, A. Gallo, L. Pastena, F. Balic, J. Quintana Fernández, D. Giordano, and D. Signorino. Monitoring a dc train supplied by a reversible substation. In *2020 IEEE International Instrumentation and Measurement Technology Conference (I2MTC)*, pages 1–6, 2020. doi: 10.1109/I2MTC43012.2020.9128644.

[22] EN 50163:2004-11. Railway applications - Supply voltages of traction systems . Standard, CEI-CT9, CEI-SC9C, 2006.

[23] G. Crotti, D. Giordano, D. Signorino, A. Delle Femine, D. Gallo, C. Landi, M. Luiso, A. Biancucci, and L. Donadio. Monitoring energy and power quality on board train. In *2019 IEEE 10th International*

Workshop on Applied Measurements for Power Systems (AMPS), pages 1–6, 2019. doi: 10.1109/AMPS.2019.8897794.

[24] EN 50463-2:2018. Railway applications - Energy measurement on board trains - Part 2: Energy measuring . Standard, CEI-CT9, April 2018.

[25] JeeHo Lee, Hyeongcheol Lee, and Jaeho Kwak. A study for improvement performance of electric brake for electric train. In *2008 International Conference on Control, Automation and Systems*, pages 1345–1348, 2008. doi: 10.1109/ICCAS.2008.4694353.

[26] Philipp Spichartz and Constantinos Sourkounis. Influence of the braking system and the type of regenerative braking request on the energy consumption of electric vehicles. In *2020 Fifteenth International Conference on Ecological Vehicles and Renewable Energies (EVER)*, pages 1–7, 2020. doi: 10.1109/EVER48776.2020.9242939.

[27] Hanmin Lee. A study on braking system using fully electric brake system. In *2014 IEEE International Conference on Industrial Technology (ICIT)*, pages 155–157, 2014. doi: 10.1109/ICIT.2014.6894930.

[28] International Organization for Standardization. *Guide to the expression of uncertainty in measurement, Supported by BIPM, IEC, IFCC, ISO IUPAC, IUPAP and OIML*. Geneva, 2008.